

# Ring-beam driven maser instability for quasiperpendicular shocks

Peter H. Yoon<sup>a)</sup>

*Institute for Physical Science and Technology, University of Maryland, College Park, Maryland 20742*

C. B. Wang<sup>b)</sup> and C. S. Wu<sup>c)</sup>

*CAS Key Laboratory of Basic Plasma Physics, School of Earth and Space Sciences, University of Science and Technology of China, Hefei, Anhui 230026, China*

(Received 8 November 2006; accepted 8 January 2007; published online 15 February 2007)

The cyclotron maser instability is a well-known radiation emission mechanism responsible for radio emissions in magnetized planets and for laboratory microwave generation devices. The present paper discusses mechanisms and properties of cyclotron maser instability driven by a ring-beam distribution of energetic electrons with application to the quasiperpendicular collisionless shock. It is shown that the fast extraordinary and ordinary electromagnetic waves as well as slow upper-hybrid Z-mode are excited over a wide range of physical parameters. The implications of the present findings for actual applications including the coronal type II radio source are also discussed. © 2007 American Institute of Physics. [DOI: 10.1063/1.2437118]

## I. INTRODUCTION

Cyclotron maser instability is a well-known radiation emission mechanism with application for radio emissions in magnetized planets including the Earth's auroral kilometric radiation (AKR),<sup>1</sup> and for laboratory microwave generation devices.<sup>2</sup> The discovery of the cyclotron maser mechanism was independently made by Twiss,<sup>3</sup> Schneider,<sup>4</sup> and Gaponov.<sup>5</sup> Their idea was taken up by the laboratory community as an inspiration for the microwave generation mechanism, and the first successful microwave device called the gyrotron was constructed in the Soviet Union in the 1960s. For an excellent up-to-date introduction to the physics of gyrotrons, the reader is referred to the recent monograph by Nusinovich.<sup>2</sup>

Although the idea of the electron cyclotron maser was known in the laboratory community for some time, the application of the concept to the natural space plasma environment was not made until the late 1970s when Wu and Lee provided the essential explanation for the Earth's AKR in terms of the cyclotron maser instability.<sup>1</sup> The research on the maser instability flourished in the 1980s, and as a result, detailed understanding of the cyclotron maser instability has been achieved. However, the interest in the subject is ongoing as recent publications testify. For instance, Farrell and Desch discuss the possible application of the maser instability to extrasolar planets;<sup>6</sup> Ergun *et al.* reinvestigate the AKR in light of the recent FAST satellite observation;<sup>7</sup> Pottelette *et al.* extend the traditional maser instability analysis to include the impact of the electron phase space holes in an effort to explain the fine structure emission;<sup>8</sup> Farrell proposes a direct O-mode maser as an alternative emission mechanism for type II radio bursts;<sup>9</sup> Vorgul *et al.* investigate the maser excitation in inhomogeneous cylindrical geometry;<sup>10</sup> Wu and

co-workers recently proposed the maser as an alternative radiation mechanism for type III solar radio bursts with sources embedded in active regions characterized by strong magnetic field;<sup>11</sup> Bingham *et al.* analyze cyclotron maser radiation from astrophysical shocks;<sup>12</sup> Begelman *et al.* suggest the maser as a possible emission mechanism for blazar jets.<sup>13</sup>

In the present discussion, we consider the maser excitation at a quasiperpendicular collisionless shock (see Ref. 12 for a related discussion). The traditionally invoked radio emission mechanism is the Langmuir wave-induced plasma emission for which the free energy source is the electron beam. However, as recent Cluster satellite observation at the Earth's bow shock shows, high-frequency electromagnetic fluctuations within the shock layer itself are primarily correlated with the loss-cone free energy source rather than the beam.<sup>14</sup> That the quasiperpendicular shock is characterized by the loss-cone (or more generally loss-cone plus the beam, also known as the "ring-beam" distribution) can be understood from the physics of quasiperpendicular collisionless shock waves.<sup>15–18</sup> Observations show that the energetic electrons and intense electromagnetic waves are generated at the quasiperpendicular shock.<sup>19–22</sup> A number of papers on the topic of shock-acceleration of energetic particles can be found in the literature.<sup>23–29</sup>

Waves associated with quasiperpendicular shocks are extensively discussed on the basis of observations made near the Earth's bow shock<sup>30,31</sup> in which the plasma frequency,  $f_p = e(n/\pi m_e)^{1/2}$ , is approximately two orders of magnitude higher than the electron gyrofrequency,  $f_c = eB/2\pi m_e c$ . Here  $e$ ,  $m_e$ ,  $c$ ,  $n$ , and  $B$  are standard symbols representing the unit charge, the electron mass, the speed of light *in vacuo*, the number density, and the ambient magnetic field intensity, respectively. The ratio  $f_p/f_c$  plays a crucial role in the theory of maser instability. For Earth's bow shock,  $f_p/f_c \propto \mathcal{O}(10^2)$ . In the low solar corona, on the other hand, this ratio can be on the order of  $\mathcal{O}(1)$  to  $\mathcal{O}(10)$ . In the present discussion we are particularly interested in the high frequency electromagnetic waves emitted by the reflected electrons with the source re-

<sup>a)</sup>Electronic mail: yoonp@glue.umd.edu

<sup>b)</sup>Electronic mail: cbwang@ustc.edu.cn

<sup>c)</sup>Also at: Institute for Physical Science and Technology, University of Maryland, College Park, Maryland 20742.

gion inside the shock layer itself as well as the immediate surrounding such as the upstream region. If one is sufficiently far away from the shock surface, then the reflected electrons may be largely characterized by the beam feature. On the other hand, if one is interested in the immediate vicinity of the shock layer, then the proper model of the reflected electrons must be a ring-beam. The ring feature of the energetic electrons leads to the emission of cyclotron maser modes, and it is the purpose of the present discussion to address this issue. References 9 and 14 also discuss similar problems, but their discussions are limited to either the Earth's bow shock or interplanetary shock with high  $f_p/f_c$ . In particular, Ref. 14 is restricted to the electrostatic approximation.

In Sec. II, we discuss the basic physics of the quasiperpendicular shock and introduce the cold ring-beam model of electron distribution function. We then formulate the cyclotron maser linear instability theory based upon the ring-beam electron model distribution. Numerical solutions of the maser instability growth rate will be presented in Sec. III over a range of physical parameters. Finally in Sec. IV, a discussion is given on the implications of the results for actual applications including the coronal type II radio bursts.

## II. BASIC CONSIDERATIONS AND PHYSICAL MODEL

In what follows, we work in the de Hoffmann-Teller (HTF) frame<sup>32</sup> moving with a velocity along the shock front such that the upstream flow velocity  $\mathbf{v}_s$  becomes parallel to the upstream magnetic field and its magnitude is given by  $v_s = v_1 / \cos \theta_{nB}$ , where  $v_1$  denotes the upstream flow velocity in the normal incident frame (NIF). Here  $\theta_{nB}$  stands for the angle between the shock normal  $\hat{\mathbf{n}}$  and the upstream magnetic field  $\mathbf{B}_1$ . Quasiperpendicular shock refers to the situation where  $\theta_{nB}$  is close to  $90^\circ$ . The normal incident frame (NIF) is another reference frame moving with a constant velocity along the shock surface in which the upstream flow velocity is normal to the shock surface. It should be noted that the NIF is not a convenient frame for the study of instabilities that may occur inside the shock layer since in this frame the linear stability analysis should take the dc electric field induced by the plasma motion normal to the shock surface into account. The essential advantage of working in HTF is that the induced dc electric field vanishes.

For a nearly perpendicular shock the magnitude of  $v_s$  in HTF is much higher than  $v_1$ . Because of the magnetic field gradient within the shock layer, a small fraction of the upstream electrons that are outside the loss cone in velocity space would be reflected by the magnetic mirror effect. Here we note that although the reflected electrons maintain the same flow velocity along the field line before and after the reflection in HTF, they are considerably energized in the laboratory frame. Such a process may be called the fast Fermi acceleration<sup>24</sup> or shock drift acceleration.

Two essential points should be made. First, in principle, the speed  $v_s$  can be infinitely high when  $\theta_{nB}$  approaches  $\pi/2$ , although in reality a meaningful number of reflected electrons can be found only when  $v_s$  is not too high so that there are enough electrons outside the loss cone. Second, it is im-

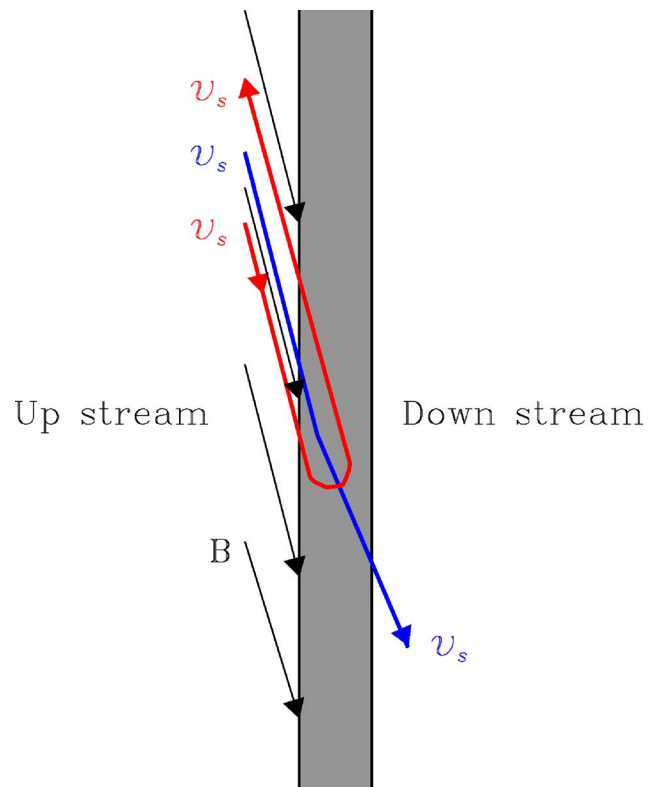


FIG. 1. The trajectories of the reflected electrons [red (gray) curve] and the core electrons [blue (black) curve] in a shock layer are schematically described in the de Hoffmann-Teller frame.

licit in the discussion of the reflection process that the electrons are moving adiabatically in the shock layer. This assumption is justified since electron gyroradii are usually small in comparison to the shock thickness.

Let us now focus our attention to the reflected electrons in HTF. As shown in Fig. 1, the upstream electrons and the reflected electrons are both moving along the field line with the same speed  $v_s$  in HTF. Of course, the parallel velocity of the reflected electrons along the magnetic field line is zero just near the reflection point such that the reflecting electrons in the vicinity of the peak magnetic field are basically a ring distribution in HTF. However, it is necessary to point out that the core electrons (or the background electrons) are not reflected and maintain approximately the same speed  $v_s$  moving along the same direction as the motion of the upstream electrons in HTF. If we denote the thickness of the shock layer by  $L_s$ , the typical time for the plasma to pass through this layer is

$$\tau \sim \frac{L_s}{v_i} \approx \frac{1}{\Omega_i},$$

where  $v_i$  is the upstream velocity and  $\Omega_i$  is the proton cyclotron frequency. If we restrict our discussion to a time scale much shorter than  $\tau$ , then we may treat the plasma in the shock as if it is homogeneous. We postulate that this condition would be satisfied under some constraint, and later justify it. Thus, if we are working in the plasma frame within HTF, the more appropriate model of the reflected electron distribution would be a ring-beam,

$$F_r = \frac{n_r}{2\pi p_\perp} \delta(p_\perp - p_{\perp 0}) \delta(p_\parallel - p_{\parallel 0}), \quad (1)$$

where  $n_r$  is the density of the reflected electrons, and  $\mathbf{p} = \gamma m_e \mathbf{v}$ ,  $m_e$  is the electron mass and  $\gamma = 1/\sqrt{1-v^2/c^2} = \sqrt{1+p^2/m_e^2 c^2}$  is the relativistic mass factor. In the above  $p_{\perp 0}$  and  $p_{\parallel 0}$  are related to  $v_s$  by  $p_{\perp 0}^2 + p_{\parallel 0}^2 \approx 2(\gamma m_e v_s)^2$ . Note that  $p_{\perp 0} \approx p_{\parallel 0} \approx \gamma m_e v_s$  is near the reflection point. Note that Eq. (1) represents the so-called ‘‘cold’’ ring-beam distribution. It is possible to include finite velocity spread in the model.<sup>12</sup> However, for the sake of simplicity, we adopt the above model. Physical justification for such a model is that the upstream velocity  $v_s$  in many applications is much higher than the electron thermal speed. Hereafter, we postulate that the wavelength is much shorter than the shock layer thickness, so the plasma can be considered as quasiuniform. The distribution function for the core electrons may be described by

$$F_0 = \frac{n_0}{2\pi p_\perp} \delta(p_\perp) \delta(p_\parallel). \quad (2)$$

Assuming that the ambient magnetic field vector is directed along the  $z$  axis and that the wave vector lies in the  $xz$  plane at an angle  $\theta$  with respect to the magnetic field vector, the  $x$  axis is in the shock normal direction, and the general form of the linear wave dispersion relation can be expressed in terms of the dielectric tensor elements  $\epsilon_{ij}$  and the index of refraction  $N = ck/\omega$  as follows:

$$0 = AN^4 - BN^2 + C, \quad (3)$$

$$A = \sin^2 \theta \epsilon_{xx} + \cos^2 \theta \epsilon_{zz} + 2 \sin \theta \cos \theta \epsilon_{xz},$$

$$B = A \epsilon_{yy} + \epsilon_{xx} \epsilon_{zz} - \epsilon_{xz}^2 + (\sin \theta \epsilon_{xy} - \cos \theta \epsilon_{yz})^2,$$

$$C = \epsilon_{xx} \epsilon_{yy} \epsilon_{zz} + \epsilon_{xx} \epsilon_{yz}^2 + \epsilon_{zz} \epsilon_{xy}^2 - \epsilon_{yy} \epsilon_{xz}^2 + 2 \epsilon_{xy} \epsilon_{yz} \epsilon_{xz}.$$

The dielectric tensor  $\epsilon_{ij}$  is comprised of the vacuum term  $\delta_{ij}$  and the plasma part represented by the susceptibility tensor  $\chi_{ij}$ , which is in turn made of two parts, one from the core electrons (denoted by subscript 0) and the second part from the reflected electrons (with subscript  $r$ ):

$$\epsilon_{ij} = \delta_{ij} + \chi_{ij}^0 + \chi_{ij}^r. \quad (4)$$

Since the cold electron contribution to  $\chi_{ij}$  can be considered as a special case of  $\chi_{ij}^r$  when  $n_r$  is simply replaced by  $n_0$  and when  $\mathbf{p}_0$  is set equal to zero, we henceforth consider only the reflected electron contribution to  $\chi_{ij}$ . Defining the total plasma frequency  $\omega_p = \sqrt{4\pi n_e e^2/m_e}$ , where  $n_t = n_r + n_0$  is the total density; the electron gyrofrequency  $\omega_c = eB/m_e c$ ; the relativistic mass factor  $\gamma = 1/\sqrt{1-\beta_\perp^2 - \beta_\parallel^2}$ , where  $\beta_\perp = p_{\perp 0}/m_e c \gamma$  and  $\beta_\parallel = p_{\parallel 0}/m_e c \gamma$ , we have (see e.g., Ref. 33)

$$\chi_{xx}^r = -\frac{n_r \Omega_p^2}{n_t \omega^2} \sum_{s=-\infty}^{\infty} \frac{s^2}{b^2} \left( b [J_s^2(b)]' \frac{a}{d_s} - \beta_\perp^2 J_s^2(b) \frac{f}{d_s^2} \right),$$

$$\chi_{yy}^r = -\frac{n_r \Omega_p^2}{n_t \omega^2} \sum_{s=-\infty}^{\infty} \left( \frac{\{b^2 [J_s'(b)]^2\}' a}{b} \frac{a}{d_s} - \beta_\perp^2 [J_s'(b)]^2 \frac{f}{d_s^2} \right),$$

$$\chi_{zz}^r = -\frac{n_r \Omega_p^2}{n_t \omega^2} - \frac{n_r \Omega_p^2}{n_t \omega^2} \sum_{s=-\infty}^{\infty} \frac{\beta_\parallel}{\beta_\perp} \left[ \left( 2b J_s^2(b) \cot \theta + \frac{\beta_\parallel}{\beta_\perp} s b [J_s^2(b)]' \right) \frac{\Omega_c}{d_s} - \beta_\perp \beta_\parallel J_s^2(b) \frac{f}{d_s^2} \right], \quad (5)$$

$$\chi_{xy}^r = -\frac{i n_r \Omega_p^2}{n_t \omega^2} \sum_{s=-\infty}^{\infty} \left( \frac{s [b J_s(b) J_s'(b)]' a}{b} \frac{a}{d_s} - \beta_\perp^2 \frac{s J_s(b) J_s'(b) f}{b} \frac{f}{d_s^2} \right),$$

$$\chi_{xz}^r = -\frac{n_r \Omega_p^2}{n_t \omega^2} \sum_{s=-\infty}^{\infty} s \left[ \left( J_s^2(b) \cot \theta + \frac{\beta_\parallel}{\beta_\perp} s [J_s^2(b)]' \right) \times \frac{\Omega_c}{d_s} - \beta_\perp \beta_\parallel \frac{J_s^2(b) f}{b} \frac{f}{d_s^2} \right],$$

$$\chi_{yz}^r = \frac{i n_r \Omega_p^2}{n_t \omega^2} \sum_{s=-\infty}^{\infty} \left[ \left( b J_s(b) J_s'(b) \cot \theta + \frac{\beta_\parallel}{\beta_\perp} s [b J_s(b) J_s'(b)]' \right) \times \frac{\Omega_c}{d_s} - \beta_\perp \beta_\parallel J_s(b) J_s'(b) \frac{f}{d_s^2} \right],$$

where

$$a = \omega - ck \beta_\parallel \cos \theta, \quad b = \frac{ck \beta_\perp}{\Omega_c} \sin \theta, \quad (6)$$

$$d_s = a - s \Omega_c, \quad f = \omega^2 - c^2 k^2 \cos^2 \theta.$$

In the above, the quantities  $\Omega_p$  and  $\Omega_c$  are relativistic plasma frequency and electron gyrofrequency, defined respectively by  $\Omega_p^2 = \omega_p^2/\gamma$  and  $\Omega_c = \omega_c/\gamma$ , and  $J_s(b)$  is the Bessel function of the first kind of order  $s$ . The off-diagonal elements satisfy the Onsager relation,  $\chi_{yx}^r = -\chi_{xy}^r$ ,  $\chi_{zy}^r = -\chi_{yz}^r$ , and  $\chi_{zx}^r = \chi_{xz}^r$ . The dielectric susceptibility associated with the cold background component can be obtained from the above by simply taking  $\beta_\perp = 0 = \beta_\parallel$  and replacing  $n_r$  by  $n_0$ ,

$$\chi_{xx}^0 = \chi_{yy}^0 = -\frac{\omega_p^2}{\omega^2 - \omega_c^2}, \quad \chi_{xy}^0 = -\chi_{yx}^0 = \frac{i \omega_c}{\omega} \chi_{xx}^0, \quad \chi_{zz}^0 = -\frac{\omega_p^2}{\omega^2}, \quad (7)$$

all other elements being zero.

In what follows, let us pay attention to the propagation angle  $\theta = 90^\circ$ . We are mainly interested in the radiation roughly parallel to the shock normal angle since the radiation propagating along the shock layer may not be observable. We also assume that the number density associated with the reflected electrons is much smaller than the background electrons ( $n_r \ll n_0$ ) such that the wave dispersion relation is largely determined by the background component. Under these assumptions, the wave dispersion relations for plasma normal modes are easily obtained in terms of either the ordinary (O) or fast/slow extraordinary (X/Z) modes. To compute the growth rate of the reactive ring-beam maser instability, we simplify the analysis by first retaining only those terms in  $\chi_{ij}^r$  that are inversely proportional to  $d_s^2$ . Then, we impose the single-harmonic approximation and retain only the  $s$ th harmonic term in the infinite harmonic series. Thirdly,

we assume that the given wave mode simultaneously satisfies the resonance condition  $\omega = s\Omega_c$  and either the O-mode or X/Z-mode dispersion relation,  $\omega = \omega_O$  or  $\omega = \omega_{X/Z}$ , where  $\omega_O$  and  $\omega_{X/Z}$  are defined, respectively, by

$$\omega_O^2 = \omega_p^2 + c^2k^2, \quad (8)$$

$$\omega_{X/Z}^2 = \frac{1}{2}(2\omega_p^2 + \omega_c^2 + c^2k^2 \pm \sqrt{(\omega_c^2 - c^2k^2)^2 + 4\omega_p^2\omega_c^2}).$$

The growth rate of the instability in the vicinity of the intersection between the cyclotron resonance  $\omega = s\Omega_c$  and the background dispersion relation  $\omega = \omega_O$  or  $\omega = \omega_{X/Z}$  can be computed if we allow a small deviation from the exact value  $\omega$ , i.e., if we let  $\omega \rightarrow \omega + \delta\omega$  and solve for  $\delta\omega$ . Interpreting the imaginary part of  $\delta\omega$  as the growth rate,  $\text{Im}(\delta\omega) \equiv \gamma$ , one arrives at the expressions for the O-mode instability growth rate,

$$\frac{\gamma_O}{\omega_c} = \frac{\sqrt{3}}{2} \left( \frac{n_r \alpha^2 \beta_{\parallel}^2}{n_0 2\gamma^2} s J_s^2(b_s) \right)^{1/3}, \quad (9)$$

$$\alpha = \frac{\omega_p}{\omega_c}, \quad b_s = \beta_{\perp} (s^2 - \gamma^2 \alpha^2)^{1/2},$$

where  $s$  must satisfy the condition  $s > \gamma\omega_p/\omega_c$  in order for  $b_s$  to be positive and real, and the X/Z-mode instability growth rate,

$$\frac{\gamma_{X/Z}}{\omega_c} = \frac{\sqrt{3}}{2} \left\{ \frac{n_r \alpha^2 \beta_{\perp}^2}{n_0 2\gamma} \frac{1}{z(2z^2 - 2\alpha^2 - \kappa^2 - 1)} \left[ \alpha^2(z^2 - \alpha^2 - \kappa^2) \right. \right. \\ \left. \left. \times \frac{s^2 J_s^2(b_s)}{b_s^2} + z^2(z^2 - \alpha^2 - 1)[s J_s'(b_s)]^2 \right. \right. \\ \left. \left. + 2z\alpha^2 \frac{s J_s(b_s) J_s'(b_s)}{b_s} \right] \right\}^{1/3}, \quad (10)$$

$$z = \frac{s}{\gamma}, \quad \kappa = \left( \frac{(z^2 - \alpha^2)^2 - z^2}{z^2 - \alpha^2 - 1} \right)^{1/2}, \quad b_s = \kappa \beta_{\perp} \gamma.$$

In the above, we must ensure that  $b_s$  remains positive and real. If a given mode number  $s$  violates this constraint, then we exclude such an  $s$  in the numerical computation. The mode designation of either X or Z depends on whether the wave frequency is on the fast extraordinary branch or the slow branch, and whether the wave is super- or subluminal (meaning slower than light speed). Specifically, the fast X mode must satisfy the conditions

$$s > \frac{\gamma}{\sqrt{2}} \sqrt{2\alpha^2 + 1 + (4\alpha^2 + 1)^{1/2}}, \quad \kappa < z, \quad (11)$$

while the slow Z mode must satisfy

$$\frac{\gamma}{\sqrt{2}} \sqrt{2\alpha^2 + 1 - (4\alpha^2 + 1)^{1/2}} < s < \gamma \sqrt{1 + \alpha^2}, \quad \kappa > z. \quad (12)$$

Of course, the maser instability driven by a ring or ring-beam distribution of energetic electrons have been discussed before,<sup>34–38</sup> but the previous analyses were concerned with the situation where  $\alpha = f_p/f_c = \omega_p/\omega_c$  is sufficiently less than unity. The primary motivation for the discussions found in

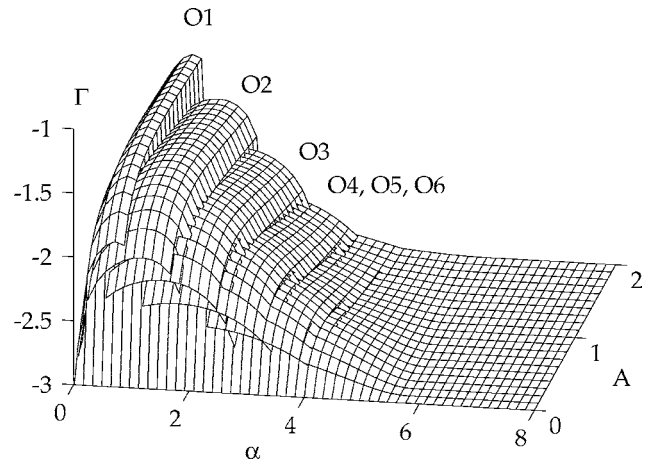


FIG. 2. Normalized O-mode growth rate  $\Gamma = (n_0/n_r)^{1/3}(\gamma_O/\omega_c)$  vs  $\alpha = \omega_p/\omega_c$  and the anisotropy factor  $A = \beta_{\parallel}/\beta_{\perp}$ , for  $\gamma = 1.05$ . Logarithmic vertical scale is employed.

the above references was on AKR and the special case of type III solar radio bursts problem where  $\alpha = \omega_p/\omega_c \ll 1$ . In contrast, the present discussion considers a wide range of the parameter  $\alpha$ .

### III. NUMERICAL RESULTS

In the numerical analysis we consider the energy of the reflected electrons such that  $\gamma \approx 1.05$ . We discuss the behavior of the ring-beam maser instability for O, X, and Z modes. Since the growth rates for these modes are simply proportional to the third power of the density ratio  $n_r/n_0$ , we discuss the numerical results in terms of the normalized growth rate  $\Gamma = (n_0/n_r)^{1/3}(\gamma/\omega_c)$ . Once  $\gamma$  is determined, then the growth rates for the plasma eigenmodes are entirely determined by two other input parameters, namely,  $\alpha = \omega_p/\omega_c$  and  $A = \beta_{\parallel}/\beta_{\perp}$ . We vary  $\alpha$  in the range  $0 < \alpha < 8$  and we consider the anisotropy factor in the range  $0 < A < 2$ . When  $A = 0$ , the distribution is a pure ring, while  $A = 1$  represents  $\beta_{\perp} = \beta_{\parallel}$ .

In Fig. 2 we plot the normalized O-mode growth rate  $\Gamma = (n_0/n_r)^{1/3}(\gamma_O/\omega_c)$  versus  $\alpha = \omega_p/\omega_c$  and the anisotropy factor  $A = \beta_{\parallel}/\beta_{\perp}$ , for  $\gamma = 1.05$ . A logarithmic vertical scale is employed. Figure 2 shows that O-mode growth rate vanishes for a pure ring distribution ( $A = \beta_{\parallel}/\beta_{\perp} = 0$ ), but for a wide range of anisotropy factor  $A$  and for a broad range of  $\alpha = \omega_p/\omega_c$ , multiple harmonic O-mode maser instability are excited (shown here are six lowest harmonics of O-mode designated by O1, O2, ..., O6), although for increasing value of  $\alpha$ , the O-mode growth rate gradually diminishes. Each harmonic  $O_n$ , where  $n = 1, 2, 3, \dots, 6$ , represents the O-mode with the frequency in the close vicinity of the  $n$ th harmonic electron cyclotron frequency.

Figure 3 displays the normalized X-mode growth rate  $\Gamma = (n_0/n_r)^{1/3}(\gamma_X/\omega_c)$  versus  $\alpha = \omega_p/\omega_c$  and  $A = \beta_{\parallel}/\beta_{\perp}$ , for the same value of  $\gamma = 1.05$ . Again, the logarithmic vertical scale is employed. According to Fig. 3, the fundamental X-mode (X1) is not excited but second and higher harmonics are excited for all ranges of  $A$  (here we plot up to the eighth harmonic). Unlike the O-mode, however, the X-mode maser

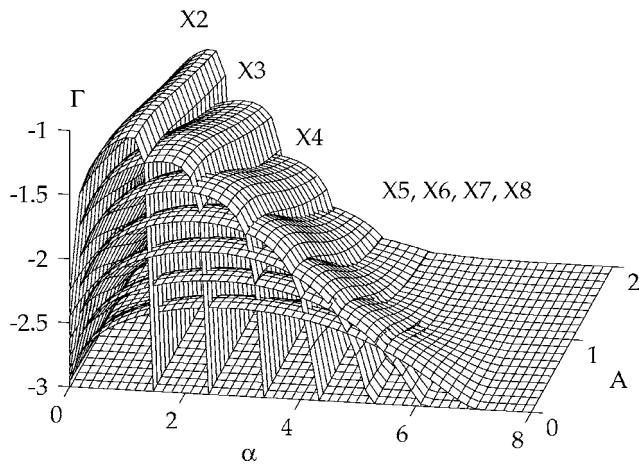


FIG. 3. Normalized X-mode growth rate  $\Gamma=(n_0/n_r)^{1/3}(\gamma_X/\omega_c)$  vs  $\alpha = \omega_p/\omega_c$  and the anisotropy factor  $A=\beta_{\parallel}/\beta_{\perp}$ , for  $\gamma=1.05$ . Logarithmic vertical scale is employed.

growth rate maximizes for  $A=\beta_{\parallel}/\beta_{\perp}=0$  for a given value of  $\alpha$ . Again, multiple harmonic X-modes are excited over a broad range of the frequency ratio  $\alpha$ . In general, the X-mode maser has a higher growth rate than the O-mode maser.

For both O- and X-modes, the growth rate of the fast electromagnetic waves eventually diminishes when  $\alpha$  becomes sufficiently high. However, the slow extraordinary mode known as the Z-mode is not affected by the increasing plasma density. The Z-mode excitation is enhanced when the upper-hybrid frequency  $\omega_{uh}=(\omega_p^2+\omega_c^2)^{1/2}$  and the  $n$ th harmonic relativistic electron cyclotron frequency  $\Omega=n\omega_c/\gamma$  coincide. As Fig. 4 shows, the growth rate of the Z-mode branch is periodically enhanced each time the condition  $\omega_{uh}\approx n\omega_c/\gamma$  is satisfied. Of course, the Z-mode cannot escape directly from the source region, but as is well-known in ionospheric physics, the slow Z-mode can escape in the form of O-mode radiation through the linear mode conversion process involving the Ellis window mechanism.<sup>39,40</sup> Another possible mechanism for radiation involving the Z-mode is

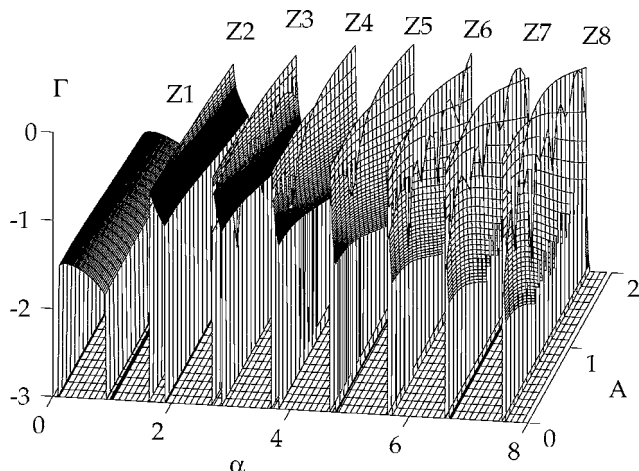


FIG. 4. Normalized Z-mode growth rate  $\Gamma=(n_0/n_r)^{1/3}(\gamma_Z/\omega_c)$  vs  $\alpha = \omega_p/\omega_c$  and the anisotropy factor  $A=\beta_{\parallel}/\beta_{\perp}$ , and for  $\gamma=1.05$ . Logarithmic vertical scale is employed.

nonlinear three-wave emerging of oppositely traveling Z modes producing electromagnetic radiation at twice the upper-hybrid frequency.<sup>41</sup>

#### IV. CONCLUSIONS AND DISCUSSION

The objective of the present research is to study a gyrotron maser instability that occurs at a quasiperpendicular shock wave. The research is motivated by the coronal type II solar radio emission, which is usually associated with solar coronal mass ejection. As generally discussed in the literature, the consensus is that the source of the observed radiation is situated inside the shock layer and its immediate upstream region. It is well known that the dynamic spectra of type II emission often exhibit herringbone and backbone structures. Researchers believe that the herringbone part is due to energetic electrons in the upstream region streaming toward higher and lower field. This picture can be envisioned if we consider a bow shock interacting with the upstream magnetic field and generating energetic electrons beaming downward and upward near the point of tangency. One may argue that the usual “plasma emission” mechanism might explain the emission. However, it is difficult to conceive that such an emission mechanism could be applied to explain the backbone part of the dynamic spectrum. To our knowledge, the issue is still not resolved.

It is important to remark that we do not claim that we have completely explained the emission mechanism of type II solar radio bursts. We only intend to point out that the cyclotron maser mechanism is a candidate that should not be overlooked. There are several advantages: (1) it does not rely on sophisticated multistep nonlinear processes while it yields direct amplification of radiation, (2) it operates in plasmas with strong ambient magnetic field, (3) it is able to explain the backbone and herringbone emissions within the same context, and (4) the physical origin of the ring-beam electrons, which are crucial for the maser mechanism is well understood.

In the present paper emphasis is placed on the analysis of maser instability due to a small population of fast electrons which possess a ring-beam distribution. As is well known, in the discussion the ratio of the plasma frequency to the electron gyrofrequency,  $f_p/f_c$ , plays an essential role in the analysis. We have shown that the fast extraordinary (X) mode, ordinary (O) mode, as well as slow extraordinary (Z) mode are excited over a wide range of the ratio of plasma frequency to electron gyrofrequency  $f_p/f_c$  and for a range of beam-to-ring anisotropy factor  $A=\beta_{\parallel}/\beta_{\perp}$ . The condition  $\beta_{\parallel}\sim\beta_{\perp}$  characterizes the inside of the shock layer, while  $\beta_{\parallel}\gg\beta_{\perp}$  is appropriate for the upstream region. If we consider the loss cone angle  $\vartheta\approx 30^\circ$ , then the upstream value of  $A=\beta_{\parallel}/\beta_{\perp}$  in HTF is about  $\sqrt{3}$ . However, in the plasma frame  $A$  should be higher. In short, although we have considered the range of  $A$  from 0 to 2, from the standpoint of practical application to low coronal type II source, we should bear in mind that only those portions corresponding to  $A>1$  is of relevance.

For relatively low values of  $f_p/f_c$ , say  $f_p/f_c$  below  $\sim 1$ , fundamental O mode (O1), second-harmonic X mode (X2),

as well as fundamental Z mode (Z1) are excited. For  $f_p/f_c$  between  $\sim 1$  and  $\sim 2$ , the most dominant wave modes are second harmonic O mode (O2) and third harmonic X mode (X3). Then over a range  $\sim 2 < f_p/f_c < \sim 3$  or so, the fastest growing modes are O3 and X4, etc. In this manner, one can see that the present discussion predicts excitation of both O and X modes over a wide range of  $f_p/f_c$ . However, when  $f_p/f_c$  is sufficiently high, say  $f_p/f_c > \sim 4$  to 5, the excitation of fast waves eventually subsides.

Here we remark that the analysis as well as the numerical results concerning growth rate discussed in the preceding paragraphs are based upon a model in which we have invoked the approximation that the plasma is homogeneous. Let us now define a threshold value  $\Gamma_0$  such that

$$\Gamma_0 \equiv \left( \frac{n_0}{n_r} \right)^{1/3} \frac{m_e}{m_p},$$

where  $m_e$  and  $m_p$  denote electron and proton masses, respectively. It is clear that our theoretical discussion is meaningful only for the case in which the normalized growth rate  $\Gamma$  is much greater than this threshold value. For example, in the case  $n_0/n_r \approx 10^3$ , the threshold value is  $\sim 10^{-2}$ . On the basis of the above discussion growth rate of any mode with  $\Gamma \leq 10^{-3}$  are insignificant and misleading. For this reason, we had eliminated all higher harmonic O and X mode whose normalized growth rate  $\Gamma$  is less than  $10^{-3}$ .

In contrast to fast O and X modes, the upper-hybrid Z mode waves are continuously excited for high values of  $f_p/f_c$ . The Z-mode excitation occurs intermittently as  $f_p/f_c$  increases, however. The instability of Z mode takes place only when the upper-hybrid matching condition  $f_{uh} = n f_c$  is met. The implication is that the Z-mode emission will be inherently structured. This finding may be highly relevant to the so-called herringbone emission structure of the solar type II bursts.

The escape of Z mode to O mode radiation may occur as a result of the Ellis radio window mechanism, which is a linear mode conversion process. The nonlinear conversion of two oppositely traveling Z modes may produce electromagnetic radiation at twice the upper-hybrid frequency. The traditional interpretation of the bow shock radiation is the beam-driven Langmuir waves that partially convert to electromagnetic radiation by means of either the linear or nonlinear mode conversion process.<sup>42</sup> The present study shows that in the presence of perpendicular free energy source, i.e., the ring feature, the quasiperpendicular propagation of the Z-mode maser may also come into play and compete with the Langmuir waves over the available free energy. In short, in the study of radio emission at the quasiperpendicular shock wave, it is important to consider the detailed phase space information of the energized electrons into theoretical discussion of the instability.

## ACKNOWLEDGMENTS

The research at the University of Maryland was supported by the NSF under Grant No. ATM0535821. The research at the University of Science and Technology of China

was supported in part by the National Nature Science Foundation of China under Grant Nos. 40474054 and 40336052, and in part by the Chinese Academy of Sciences under Grant No. KZCX3-SW-144.

- <sup>1</sup>C. S. Wu and L. C. Lee, *Astrophys. J.* **230**, 621 (1979).
- <sup>2</sup>G. S. Nusinovich, *Introduction to the Physics of Gyrotrons* (The Johns Hopkins University, Baltimore, 2004).
- <sup>3</sup>R. Q. Twiss, *Aust. J. Phys.* **11**, 564 (1958).
- <sup>4</sup>J. Schneider, *Phys. Rev. Lett.* **2**, 504 (1959).
- <sup>5</sup>A. V. Gaponov, *Izv. Vyssh. Uchebn. Zaved., Radiofiz.* **2**, 450 (1959) (in Russian).
- <sup>6</sup>W. M. Farrell and M. D. Desch, *J. Geophys. Res.* **104**, 14025 (1999).
- <sup>7</sup>R. E. Ergun, C. W. Carlson, J. P. McFadden, G. T. Delory, R. J. Strangeway, and P. L. Pritchett, *Astrophys. J.* **538**, 456 (2000).
- <sup>8</sup>R. Pottelette, R. A. Treumann, and M. Berthomier, *J. Geophys. Res.* **106**, 8465 (2001).
- <sup>9</sup>W. M. Farrell, *J. Geophys. Res.* **106**, 15701 (2001).
- <sup>10</sup>I. Vorgul, R. A. Cairns, and R. Bingham, *Phys. Plasmas* **12**, 122903 (2005).
- <sup>11</sup>C. S. Wu, C. B. Wang, G. C. Zhou, S. Wang, and P. H. Yoon, *Astrophys. J.* **621**, 1129 (2005).
- <sup>12</sup>R. Bingham, B. J. Kellett, R. A. Cairns, J. Tongue, and J. T. Mendonca, *Astrophys. J.* **595**, 279 (2003).
- <sup>13</sup>M. C. Begelman, R. E. Ergun, and M. J. Rees, *Astrophys. J.* **625**, 51 (2005).
- <sup>14</sup>V. V. Lobzin, V. V. Krasnoselskikh, S. J. Schwartz, I. Cairns, B. Lefebvre, P. Décréau, and A. Fazakerley, *Geophys. Res. Lett.* **32**, L18101 (2005).
- <sup>15</sup>D. A. Tidman and N. A. Krall, in *Shock Waves in Collisionless Plasmas* (Wiley-Interscience, New York, 1971).
- <sup>16</sup>D. Biskamp, *Nucl. Fusion* **13**, 419 (1973).
- <sup>17</sup>V. Formisano, *J. Phys. (Paris)* **38**, C6 (1977).
- <sup>18</sup>E. W. Greenstadt and R. W. Fredricks, in *Space Plasma Physics: The Study of Solar-System Plasmas, 2* (National Academy of Sciences, Washington, D.C., 1979), p. 807.
- <sup>19</sup>K. A. Anderson, R. P. Lin, F. Martel, C. S. Lin, G. K. Parks, and H. Réme, *Geophys. Res. Lett.* **6**, 401 (1979).
- <sup>20</sup>K. A. Anderson, *J. Geophys. Res.* **86**, 4445 (1981).
- <sup>21</sup>G. K. Parks, E. Greenstadt, C. S. Wu, C. S. Lin, A. St.-Marc, R. P. Lin, K. A. Anderson, C. Gurgiolo, B. Mauk, H. Réme, R. Anderson, and T. Eastman, *J. Geophys. Res.* **86**, 4343 (1981).
- <sup>22</sup>A. J. Klimas, in *Collisionless Shocks in the Heliosphere, Geophys. Monograph Series 35*, edited by B. T. Tsurutani and R. G. Stone (AGU, Washington, 1985), p. 237.
- <sup>23</sup>D. W. Potter, *J. Geophys. Res.* **86**, 11111 (1981).
- <sup>24</sup>C. S. Wu, *J. Geophys. Res.* **89**, 8857 (1984).
- <sup>25</sup>M. M. Leroy and A. Mangeney, *Ann. Geophys. (Gauthier-Villars, 1983-1985)* **2**, 449 (1984).
- <sup>26</sup>D. Krauss-Varban and D. Burgess, *J. Geophys. Res.* **96**, 143 (1991).
- <sup>27</sup>D. Krauss-Varban and C. S. Wu, *J. Geophys. Res.* **94**, 15367 (1989).
- <sup>28</sup>D. Krauss-Varban, *J. Geophys. Res.* **99**, 2537 (1994).
- <sup>29</sup>M. Vandas, *J. Geophys. Res.* **106**, 1859 (2001).
- <sup>30</sup>C. S. Wu, D. Winske, Y. M. Zhou, S. T. Tsai, P. Rodriguez, M. Tanaka, K. Papadopoulos, K. Akimoto, C. S. Lin, M. M. Leroy, and C. C. Goodrich, *Space Sci. Rev.* **37**, 63 (1984).
- <sup>31</sup>J. D. Scudder, A. Mangeney, C. Lacombe, C. C. Harvey, and T. L. Aggson, *J. Geophys. Res.* **91**, 11075 (1986).
- <sup>32</sup>G. K. Parks, *Physics of Space Plasmas* (Addison-Wesley, New York, 1991), pp. 413–458.
- <sup>33</sup>D. B. Melrose, *Instabilities in Space and Laboratory Plasmas* (Cambridge University Press, New York, 1986), pp. 163–208.
- <sup>34</sup>K. R. Chu and J. L. Hirshfield, *Phys. Fluids* **21**, 461 (1978).
- <sup>35</sup>R. M. Winglee, *Plasma Phys.* **25**, 217 (1983).
- <sup>36</sup>P. L. Pritchett, *J. Geophys. Res.* **89**, 8957 (1984).
- <sup>37</sup>R. J. Strangeway, *J. Geophys. Res.* **90**, 9675 (1985).
- <sup>38</sup>Y. P. Chen, C. B. Wang, and G. C. Zhou, *Acta Phys. Sin.* **54**, 3221 (2005).
- <sup>39</sup>G. R. Ellis, *J. Atmos. Terr. Phys.* **8**, 43 (1956).
- <sup>40</sup>M. S. Smith, *Nature (London), Phys. Sci.* **243**, 29 (1973).
- <sup>41</sup>D. B. Melrose, *Astrophys. J.* **380**, 256 (1991).
- <sup>42</sup>I. H. Cairns, P. A. Robinson, and G. P. Zanks, *Publ. - Astron. Soc. Aust.* **17**, 22 (2000).